ORIGINAL PAPER

Electrochemical properties of nano-crystalline LiNi$_{0.5}$Mn$_{1.5}$O$_4$ synthesized by polymer-pyrolysis method

Lifen Xiao · Yanqiang Zhao · Yanyan Yang ·
Xinping Ai · Hanxi Yang · Yuliang Cao

Abstract LiNi$_{0.5}$Mn$_{1.5}$O$_4$ powders were prepared through polymer-pyrolysis method. XRD and TEM analysis indicated that the pure spinel structure was formed at around 450 °C due to the very homogeneous intermixing of cations at the atomic scale in the starting precursor in this method, while the well-defined octahedral crystals appeared at a relatively high calcination temperature of 900 °C with a uniform particle size of about 100 nm. When cycled between 3.5 and 4.9 V at a current density of 50 mA/g, the as prepared LiNi$_{0.5}$Mn$_{1.5}$O$_4$ delivered an initial discharge capacity of 112.9 mAh/g and demonstrated an excellent cyclability with 97.3% capacity retentive after 50 cycles.

Keywords LiNi$_{0.5}$Mn$_{1.5}$O$_4$ cathode · Polymer-pyrolysis · Lithium ion batteries

Introduction

Recently, spinel phase 5 V cathode materials for lithium ion batteries have attracted much attention due to their possibly high energy density, good cycle stability, low cost and toxicity. These materials are based on spinel LiMn$_2$O$_4$, where manganese is partially substituted by transition metals (LiM$_x$Mn$_{2-x}$O$_4$, M=Cr, Cu, Co, Fe, Ni, etc.) [1–6]. It has been well recognized that the 5 V plateau originates from the redox of the substituted transition metals so that the capacity and plateau voltage of the materials in the 5 V region strongly depend on the nature and the content of the transition metals. Among these materials, LiNi$_{0.5}$Mn$_{1.5}$O$_4$ delivers a dominant potential plateau around 4.7 V and 2-electron discharge capacity, resulting from the redox reaction of Ni^{2+}/Ni^{4+} couple along with the Li$^+$ ion extraction–insertion. Because the oxidation state of manganese is fixed to +4 valence, the Mn^{4+} ions in the crystalline lattice only acts as a host matrix, which can eliminate the structure distortion due to Mn^{3+} formation during cycling and therefore LiNi$_{0.5}$Mn$_{1.5}$O$_4$ shows the highest cycling stability [7]. This suggests a possible use of this material for fabrication of new generation of 5 V lithium ion batteries.

Because of the difficulties in the preparation of pure phase spinel products by traditional solid state reaction, LiNi$_{0.5}$Mn$_{1.5}$O$_4$ materials have been synthesized by various wet-chemical methods to achieve crystal homogeneity of the product. These processes include sol-gel, spray pyrolysis, emulsion drying, coprecipitation and molten salt process [7–15]. A main disadvantage of these synthetic methods is too complicated and time consuming to be easily applied in practical production. In this paper, we report a polymer-pyrolysis method [16, 17] for synthesizing nano-crystalline LiNi$_{0.5}$Mn$_{1.5}$O$_4$. In this method, the precursor compounds including Li, Ni and Mn salts is mixed homogenously at atomic scale, the formation of polyacrylate is quick and easy to control, and the final high temperature calcination duration is much shorten than other methods. Most importantly, it is advantageous to gain the pure nano-crystalline materials with uniformly distributed size.

L. Xiao (✉) · Y. Zhao · Y. Yang
College of Chemistry, HuaZhong Normal University,
Wuhan 430079, China
e-mail: lfxiao@mail.ccnu.edu.cn

X. Ai · H. Yang · Y. Cao
College of Chemistry and Molecular Science, Wuhan University,
Wuhan 430072, China

Experimental

The nanocrystalline $LiNi_{0.5}Mn_{1.5}O_4$ powders were synthesized by pyrolysis of acrylate salts of Li, Ni and Mn. In this method, stoichiometric amounts of $LiOH$, $Ni(NO_3)_2$ and $Mn(NO_3)_2$ were first dissolved in acrylic acid to form a homogeneously distributed solution of acrylate salts under stirring. Then a small amount of $(NH_4)_2S_2O_8$ as initiator and 80 °C heating for 2 h were applied to the solution to form the well-distributed polyacrylates of Li, Ni, and Mn. The resulting polyacrylate precursor was dried at 120 °C for 24 h and decomposed at 450 °C for 6 h in air to get pure Li-Ni-Mn oxides. These precalcined powders were grounded in agate mortar and recalcined between 600 and 900 °C for 3 h in air and then cooled slowly at a rate of 10 °C/min to obtain high-crystalline products of $LiNi_{0.5}Mn_{1.5}O_4$.

TG/TGA measurement was conducted on TGA Q500 thermogravimetric analyzer (TA Instruments, USA) in air at a scan rate of 10 °C/min from room temperature to 1,000 °C. Powder X-ray diffraction (XRD) was performed on Shimadzu XRD-6000 diffractometer using Cu $K\alpha$ radiation in the range of 10–80° of 2θ angles at a scan rate of 4 °C/min. The particle morphologies were examined with JEM-2010 Transition Electron Microscope (TEM).

The electrochemical properties of $LiNi_{0.5}Mn_{1.5}O_4$ were measured on the test cells of a three-electrode design. The $LiNi_{0.5}Mn_{1.5}O_4$ cathodes were prepared by roll pressing the mixed paste of 80% $LiNi_{0.5}Mn_{1.5}O_4$ powder, 8% acetylene black, and 12% PTFE (wt.%) into film and then pressing the electrode film onto aluminum net. The test electrodes have neat mass density of $LiNi_{0.5}Mn_{1.5}O_4$ in the range of 7–10 mg/cm^2. The counter electrodes and reference electrodes were lithium sheets. The separator was Celgard 2400 microporous membrane. The electrolyte was 1 mol·l^{-1} $LiPF_6$ dissolved in a 1:1:1 mixture (by weight) of ethylene carbonate, dimethyl carbonate, and ethylene methyl carbonate purchased from Shinestar battery materials Co., Ltd (China). The cells were assembled in an argon-filled glove box. The charge–discharge measurements were carried out using a BTS-55 Newware battery charger (ShenZhen, China) at a current density of 50 mA/g of $LiNi_{0.5}Mn_{1.5}O_4$. The cyclic voltammetry was carried out with CHI660A Electrochemical Workstation between 3.5 and 5.1 V vs Li/Li$^+$ reference electrode at a scan rate of 0.1 mV/s.

Results and discussion

To understand the synthetic chemistry of the material during the preparation process, the copolymeric precursor of Li-Ni-Mn polyacrylate precursor was examined by thermogravimetric analysis and the TG/TGA results between room temperature and 1,000 °C are shown in Fig. 1.

It shows that the weight loss of the copolymeric precursor occurred in three discrete steps and terminated near 410 °C. The associated peaks in the TGA curves may be attributed to the combustion of LiPA (Li polyacrylate), NiPA (Ni polyacrylate) and MnPA (Mn polyacrylate) into metallic carbonates, which were further decomposed to metallic oxides [16]. The total weight loss is 66.31%, which is in good agreement with the theoretical values of 66.1% expected from the proposed reaction schemes of P(Li,Ni, Mn; 5AA)→$LiNi_{0.5}Mn_{1.5}O_4$, indicating that the polyacrylates were formed in stoichiometry. It is noticed that there is a slight weight loss when the temperature is higher than 710 °C, which is probably caused by the loss of oxygen and lithium element. According to the TG/TGA curves, we settled the precalcination process at 450 °C to produce pure metallic oxides at first and then recalcined the low-crystalline powders at a relatively high temperature of 600, 700, 800, and 900 °C, respectively, for 3 h to optimize the calcination temperature for the best electrochemical performance of material.

Figure 2 shows the XRD patterns of the Li-Ni-Mn oxides powders obtained by precalciniation at 450 °C for 6 h and recalcined at 600, 700, 800, and 900 °C for 3 h in air. It can be seen that the samples pyrolysized even at 450 °C has already shown a rudimental cubic spinel structure, agreeing well with that investigated in the TG curve. It is found that all the peaks in the patterns become sharper and stronger with the calcination temperature increasing from 450 to 900 °C, indicating the improved crystallinity of the materials at higher calcination temperatures. According to the literature [7–8], it is very difficult to obtain a single-phase spinel product even by the sol-gel method without segregation of impurity phase such as NiO and Li_xNi_yO compound, which can deteriorate the electrochemical properties. However, as can be seen in Fig. 1, all the samples show a phase-pure cubic spinel structure, and
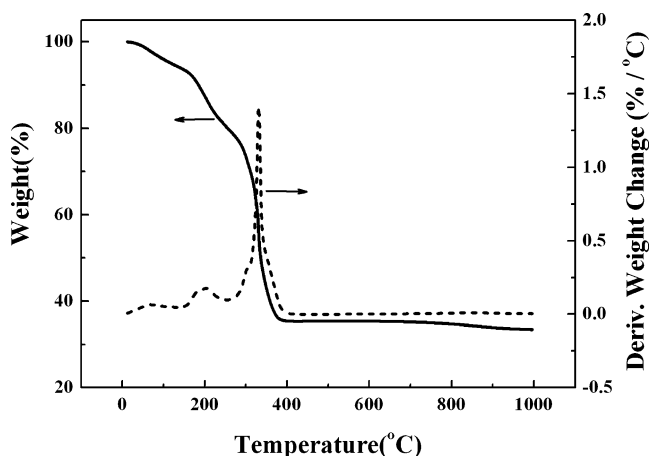

Fig. 1 TG/TGA curves of the copolymeric precursor of Li-Ni-Mn polyacrylates
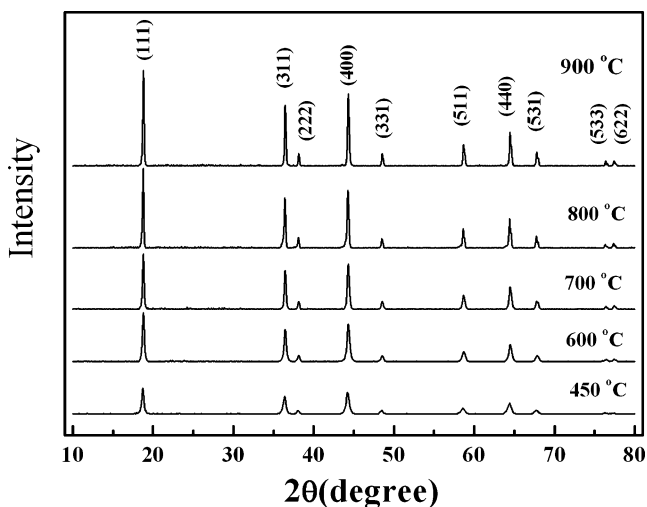
Fig. 2 XRD patterns of the $LiNi_{0.5}Mn_{1.5}O_4$ powders precalcined at 450 °C for 6 h and recalcined at 600, 700, 800, and 900 °C for 3 h

there is no sign of any impurities detected, indicating the very good incorporation of Ni atoms onto the Mn sites. This confirms that the cations, i.e., Li, Ni, and Mn ions in the starting precursor are dispersed homogenously at atomic scale, so that the perfect solid solution in the $LiNi_{0.5}Mn_{1.5}O_4$ structure can be easily formed in a broad temperature range.

The lattice parameters of $LiNi_{0.5}Mn_{1.5}O_4$ powders calculated from the XRD patterns are shown in Fig. 3. As can be seen, the lattice parameter decreases sharply from 450 to 700 °C at first, then increases slightly with increasing the calcination temperature. The decrease in the lattice parameter is probably due to the improved crystallinity of the powder at high temperature, while the increase should be owing to the generation of Mn^{3+} in the terminal product. It is known that oxygen deficiency in the product occurs at high temperatures as can be checked in the TG curve shown in Fig. 1, and thus small portion of Mn^{4+} is
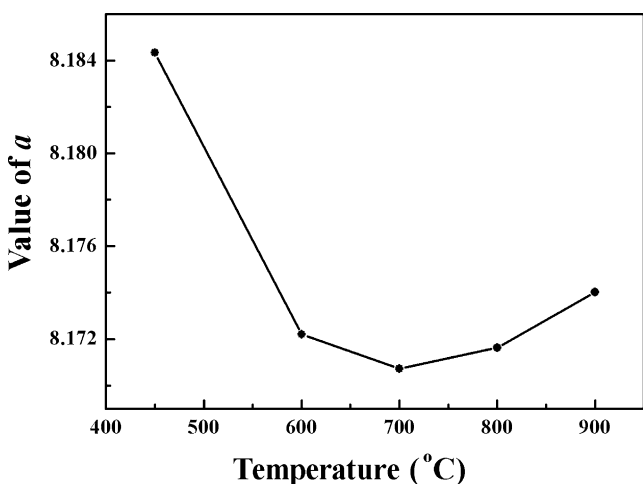
reduced to Mn^{3+} to keep the charge balance [18]. Due to the larger radii of Mn^{3+} than Mn^{4+}, the lattice parameter increases with increasing Mn^{3+} content in the final products.

Figure 4 shows the TEM image of the Li-Ni-Mn oxides powders obtained by precalcined at 450 °C for 6 h and recalcined at 900 °C for 3 h in air. It is shown that the 450 °C precalcined powders are composed of irregularly shaped and loosely conglomerated particles with broad distributed size below 50 nm. With increasing calcination temperature to 900 °C, the powders are composed of crystals of octahedral shape with defined crystal faces. Besides, the particles have grown up into individual grains and shown uniform particle distribution of ca.100 nm. Both the XRD and the TEM investigations indicate that the formation temperature of spinel phase is as low as 450 °C, whereas the growth of integrated $LiNi_{0.5}Mn_{1.5}O_4$ crystals takes place at relatively higher calcination temperature. On the other hand, due to the nucleation already occurring at a relatively low temperature, the $LiNi_{0.5}Mn_{1.5}O_4$ phase thus

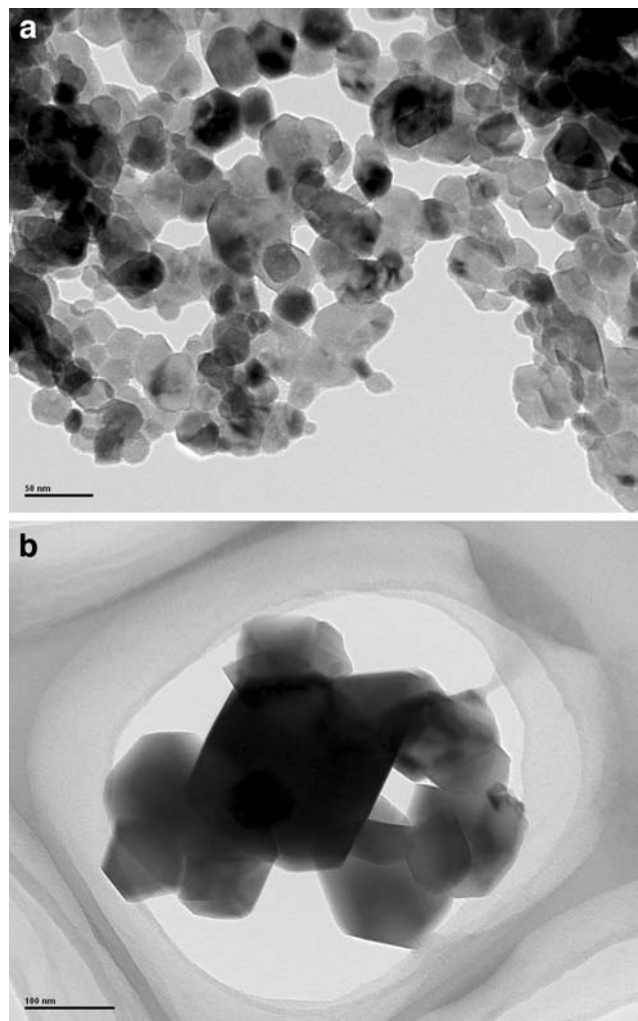**Fig. 3** the lattice parameter of $LiNi_{0.5}Mn_{1.5}O_4$ powders as a function of the calcination temperature

Fig. 4 TEM image of the $LiNi_{0.5}Mn_{1.5}O_4$ powders precalcined at 450 °C for 6 h (**a**), and recalcined at 900 °C for 3 h (**b**)
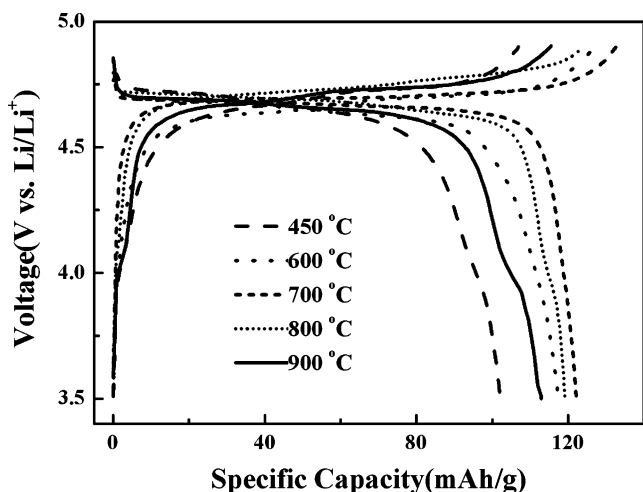
Fig. 5 charge–discharge curves of the Li/ LiNi$_{0.5}$Mn$_{1.5}$O$_4$ cells in the potential range of 3.5–4.9 V at a current density of 50 mA/g with the LiNi$_{0.5}$Mn$_{1.5}$O$_4$ powders precalcined at 450 °C for 6 h and reacalcined at 600, 700, 800, and 900°C for 3 h
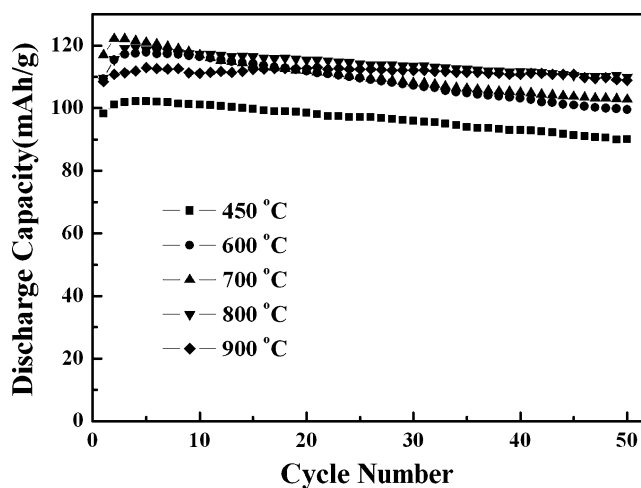

Fig. 6 cycling behavior of the Li/LiNi$_{0.5}$Mn$_{1.5}$O$_4$ cells in the potential range of 3.5–4.9 V at a current density of 50 mA/g with the LiNi$_{0.5}$Mn$_{1.5}$O$_4$ powders precalcined at 450 °C for 6 h and recalcined at 600, 700, 800, and 900°C for 3 h

produced can be easily obtained at high temperature in a very short calcination time of 3 h in our case.

The calcination temperature has significant effects on the structure and morphology of the materials so as to affect their electrochemical performance. Figure 5 shows the charge–discharge profiles of the Li/LiNi$_{0.5}$Mn$_{1.5}$O$_4$ cells in terms of calcination temperature. The cells were operated at a specific current of 50 mA/g in the voltage range of 3.5–4.9 V. As shown in Fig. 5, the discharge capacity is about 102.2, 117.4, 122.2, 119.2 and 112.8 mAh/g for the LiNi$_{0.5}$Mn$_{1.5}$O$_4$ powder calcined at 450, 600, 700, 800 and 900 °C, respectively. It can be found that with increasing calcination temperature from 450 to 700 °C, the reversible capacity first increases gradually to a maximum value at 700 °C and then decreases with increasing calcination temperature from 800 to 900 °C. This trend can be well understood by considering the change in the crystallinity of the powders with calcination temperature. The higher calcination temperature leads to higher crystallinity that helps to increase the electrode capacity. On the other hand, higher calcination temperature may produce particles with relatively large size and long diffusion distance of lithium ion, which makes lithium ion insertion–extraction difficult. Therefore, with the combination of these two factors, the powders calcined at 700 °C deliver the highest discharge capacity.

It can also be seen from Fig. 5 that the cells using LiNi$_{0.5}$Mn$_{1.5}$O$_4$ calcined at ≤700 °C exhibit only a flat voltage plateau at 4.7 V, while using LiNi$_{0.5}$Mn$_{1.5}$O$_4$ calcined at higher temperatures give additional small discharge plateau at 4 V. It is well recognized that the 4.7 V plateau is attributed to the Ni^{2+}/Ni^{4+} redox couple, while the 4.0 V plateau is related to the Mn^{3+}/Mn^{4+} redox couple. Apparently, there is a very small amount of Mn^{3+}

existing in the higher-temperature-calcined powders owing to oxygen loss, which is consistent with the increase in lattice parameter at high temperature as shown in Fig. 3. Compared with the data reported in the literature [10, 12, 14], the discharge capacity around 4.0 V is smaller, indicating that the possibility of the formation of Mn^{3+} in the cubic phase is much lower by the polymer-pyrolysis method.

Figure 6 shows the cycling performance of the Li/ LiNi$_{0.5}$Mn$_{1.5}$O$_4$ cells between 3.5 and 4.9 V at 50 mA/g. As Fig. 6 illustrates, the higher calcination temperature leads to higher cyclability. The powder calcined at 900 °C shows the best cycleability and the capacity retains 97.3% after 50 cycles. This result is consistent with the XRD and TEM data, indicating that higher crystallinity of the powders
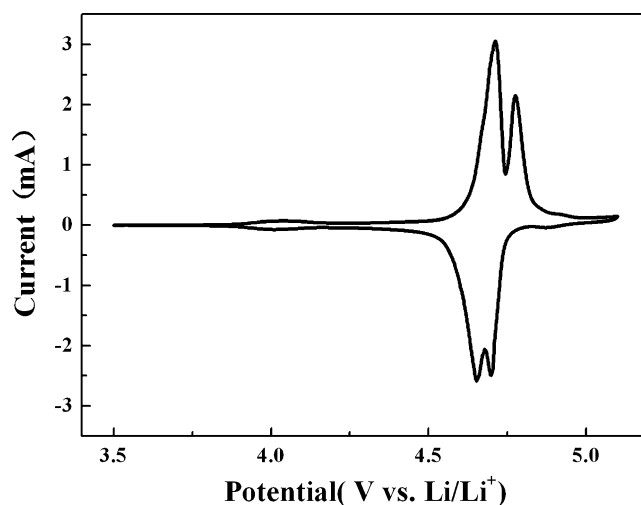

Fig. 7 Cycling Voltammograms of the LiNi$_{0.5}$Mn$_{1.5}$O$_4$ powders calcined at 900 °C for 3 h between 3.5 and 5.1 V vs. Li/Li$^+$ reference electrode at a scan rate of 0.1 mV/s

favor to remain the structure stability during repeated lithium insertion and extraction.

The cyclic voltammogram of the $LiNi_{0.5}Mn_{1.5}O_4$ powders prepared at 900 °C is presented in Fig. 7. It shows two pairs of pronounced redox peaks at around 4.5–4.8 V, which should be attributed to the progressive oxidation and reduction in Ni^{2+}/Ni^{3+}(4.712, 4.654 V) and Ni^{3+}/Ni^{4+} (4.777, 4.698 V) couples, suggesting that the capacity at the 5-V region is determined by the amount of Ni ions during the charge–discharge tests. The curve also shows a pair of very weak peaks around 4.0 V, which should be related to the redox couple of Mn^{3+}/Mn^{4+}, indicating few Mn^{3+} ions are present in the 900 °C calcined powders. As can be seen in Fig. 7, the redox peaks are very sharp and symmetrical, illustrated the very reversibility and fast kinetics of this material synthesized in this work.

Conclusion

Spinel $LiNi_{0.5}Mn_{1.5}O_4$ has been synthesized by a polymer-pyrolysis method. The structure, morphology and electrochemical properties of the powders are closely related to the calcination temperature. The charge–discharge tests show that 900 °C for 3 h calcined powders have delivered a moderate specific discharge capacity of 112.9 mAh/g and the best cycling stability during cycling voltage interval of 3.5–4.9 V with 97.3% retention after 50 cycles. Cyclic Voltammetric studies show two pairs of pronounced and sharp and symmetrical redox peaks at around 4.5–4.8 V, illustrating the very reversibility and fast kinetics on the lithium ion deintercalation–intercalation reactions of the powders. The good electrochemical performances are in good agreement with the better crystallinity of the powders prepared at such temperature, as supported by XRD, SEM measurement.

References

1. Sigala C, Guyomard D, Verbaere A, Piffard Y, Tournoux M (1995) Solid State Ion 81:167
2. Eli YE, Howard WF (1997) J Electrochem Soc 144:L205
3. Kawai H, Nagata M, Tukamoto H, West AR (1998) Electrochem Solid State Lett 1:212
4. Eftekhari A (2003) J Power Sources 124:182
5. Amine K, Tukamoto H, Yasuda H, Fujita Y (1996) J Electrochem Soc 143:1607
6. Mandal S, Rojas RM, Amarilla JM, Calle P, Kosova NV, Anufrienko VF, Rojo JM (2002) Chem Mater 14:1598
7. Zhong Q, Bonakdarpour A, Zhang M, Gao Y, Dahn JR (1997) J Electrochem Soc 144:205
8. Wu X, Kim SB (2002) J Powder Sources 109:53
9. Wu HM, Tu JP, Chen XT, Shi DQ, Zhao XB, Cao GS (2006) Electrochim Acta 51:4148
10. Myung S-T, Komaba S, Kumagai N, Yashiro H, Chung H-T, Cho T-H (2002) Electrochim Acta 47:2543
11. Ohzuku T, Ariyoshi K, Yamamoto S, Makimura Y (2001) Chem Lett 1270
12. Lee YS, Suo YK, Ota S, Miyashita T, Yoshio M (2002) Electrochem Commun 4:989
13. Kim JH, Myung ST, Sun YK (2004) Electrochim Acta 49:220
14. Wen L, Lu Q, Xu G (2006) Electrochim Acta 51:4388
15. Taniguchi T, Lim CK, Song D, Wakihara M (2002) Solid State Ion 146:239
16. Yu L, Yang H, Ai X, Cao Y (2005) J Phys Chem B 109:1148
17. Yu LH, Cao YL, Yang HX, Ai XP (2006) J Solid State Electrochem 10:283
18. Kim JH, Myung ST, Kang CS, Sun YK (2004) Chem Mater 16:906